# Co nowego w rozbłyskach słonecznych?

Barbara Sylwester
Zakład Fizyki Słońca CBK PAN

# Papers presented

- Woods et al., 2011, ApJ, 739: New solar extreme-ultraviolet irradiance observations during flares
- Hock, Woods, Klimchuk et al., 2012, ApJ: The origin of the EUV late phase: a case study of the C8.8 flare on 2010 May 5
- Chamberlin, Milligan and Woods, 2012, Solar Phys., 279: Thermal Evolution and Radiative Output of Solar Flares Observed by the EUV Variability Experiment (EVE)
- Battaglia and Kontar, 2012, ApJ, 760: *RHESSI* and *SDO*/AIA observations of the chromospheric and coronal plasma parameters during a solar flare
- Schmelz, Jenkins, and Pathak, 2013, ApJ, 770: Atmospheric imaging assembly observations of coronal loops: cross-field temperature distributions
- Cirtain, Golub, Winebarger et al., 2013, Nature, 493 : Energy release in the solar corona from spatially resolved magnetic braid

# ***S**olar **D**ynamic **O**bservatory (SDO)*

*SDO* is the first spacecraft in NASA's **L**iving **W**ith a **S**tar (LWS) program and is scheduled for a nominal five-year mission (launched on 2010 Feb. 11) to study how the Sun drives space weather and influence the Earth→

3 instruments:

**1) A**tmospheric **I**maging **A**ssembly (**AIA**): 4 telescopes, 4096x4096 pixel CCD, full-disk solar images at 7 EUV bands with 12 second cadence, 0.6 arc-seconds resolution

**2) H**elioseismic and **M**agnetic **I**mager (**HMI**) - vector magnetograph

**3) E**xtreme ultraviolet **V**ariability **E**xperiment (E**VE**) – measure disk-integrated radiance, normal operations started on 2010 May 1

→ **M**ultiple **E**UV **G**rating **S**pectrographs (**MEGS** channels): EUV spectral observations from 6 to 105 nm (70 000 K÷10 MK)

→ MEGS-A channel 7-37 nm, grazing incidence spectrograph, spectral resolution of 0.1 nm, cadence of 10 s

→ MEGS-B 37-105 nm, normal incidence, dual-pass spectrograph, reduced duty cycle - operates 3 h per day

→ **E**UV **S**pectro**P**hotometers (**ESP**): broadband observations from **0.1 to 39 nm**, cadence 0.25 s

EVE – rocket calibration flight on 3 May 2010 and in flight calibration

# *GOES* fluxes for 5 May 2010

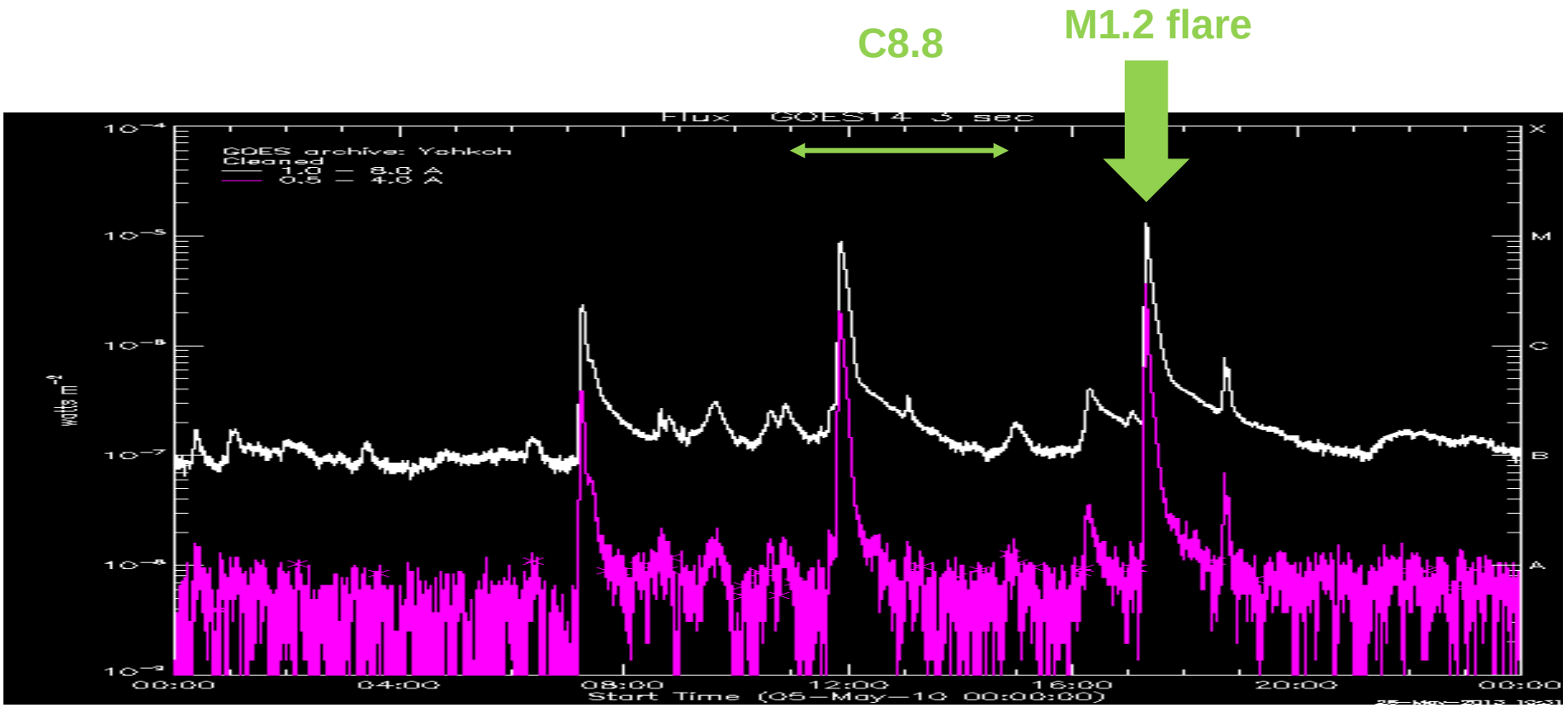

# 5 May 2010 (AIA 171 Å movie)

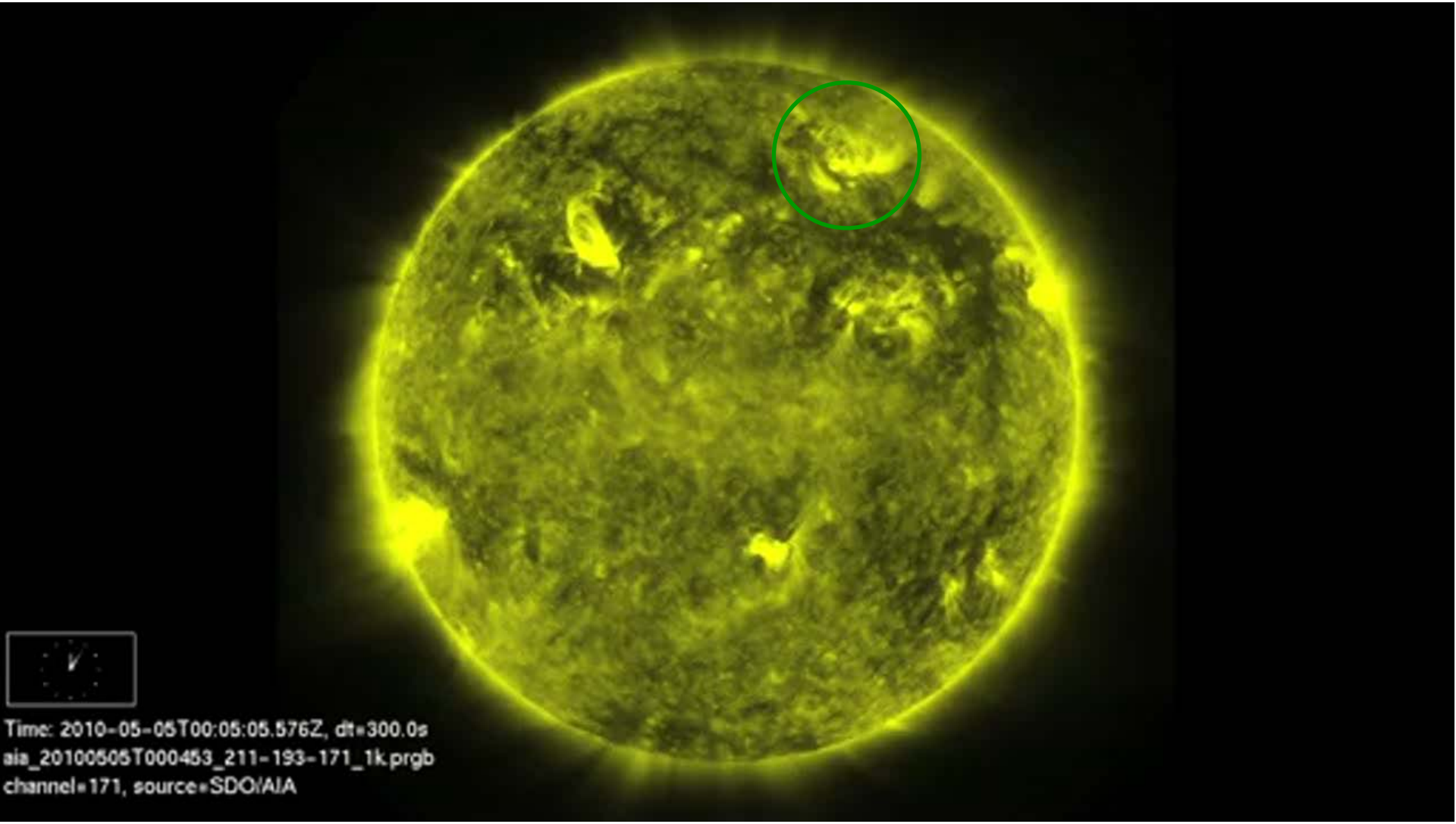

# Late phase: EVE (1st year of *SDO* operation)

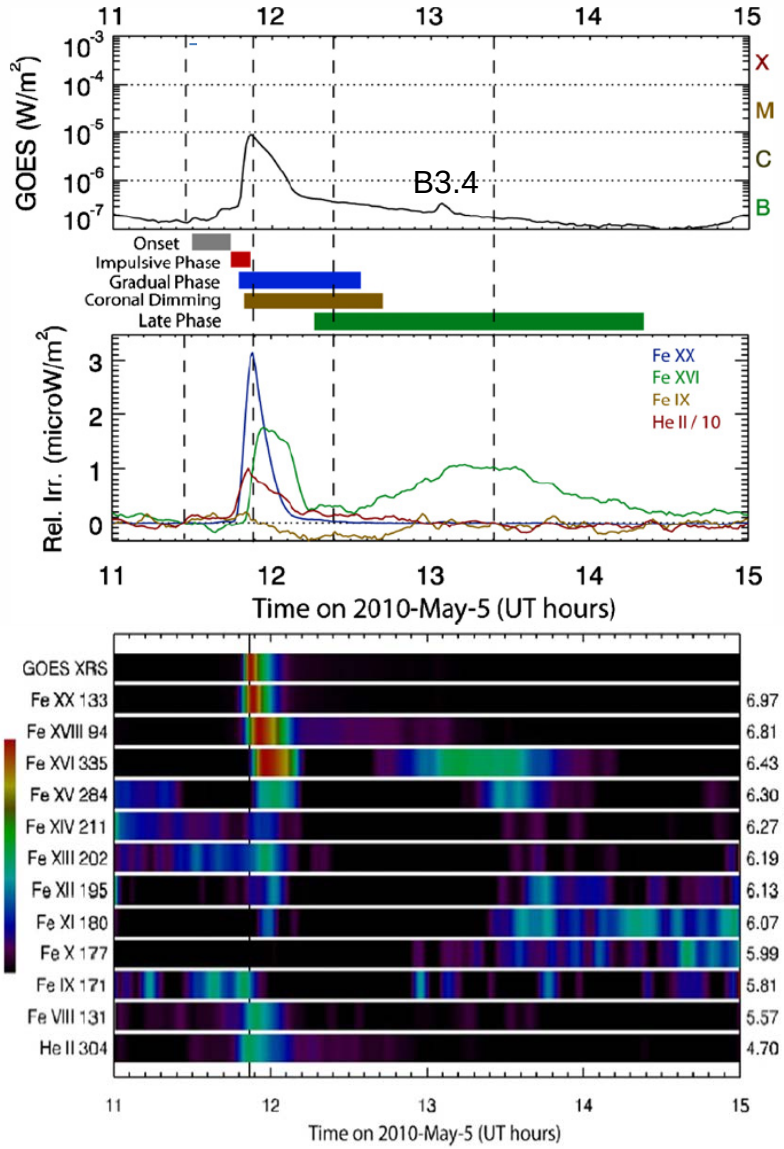


Cooling rate is much slower for EUV late phase loops than for gradual phase loops.

Relative irradiance= solar irradiance spectrum – pre-flare spectrum

**Fe XX 13.3 nm → hot corona 10-16 MK**

**Fe XVI 33.5 nm → warm corona 2-3 MK**

**Fe IX 17.1 nm → cool corona 0.7 MK**

**He II 30.4 nm → TR emission 0.08 MK**

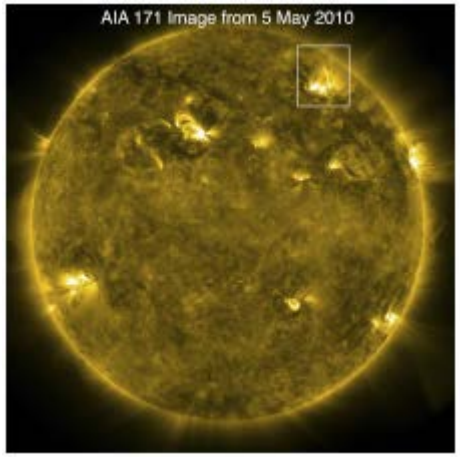


AR 11069 during C8.8 flare on 2010 May 5. Six EUV late flares have been located there.

*Woods et al., 2011, ApJ, 739*

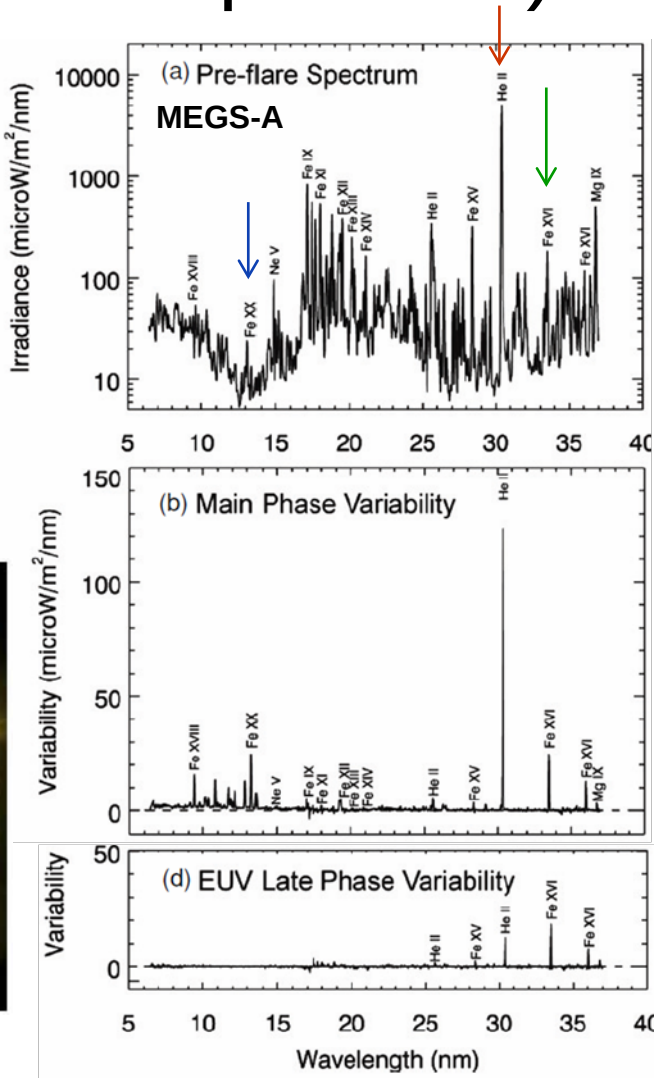


Spectral variability between pre-flare, main phase and EUV late phase. (5 minutes averages at times of vertical lines at upper left plot.)

# C8.8 flare on 2010 May 5 (AIA & EVE)

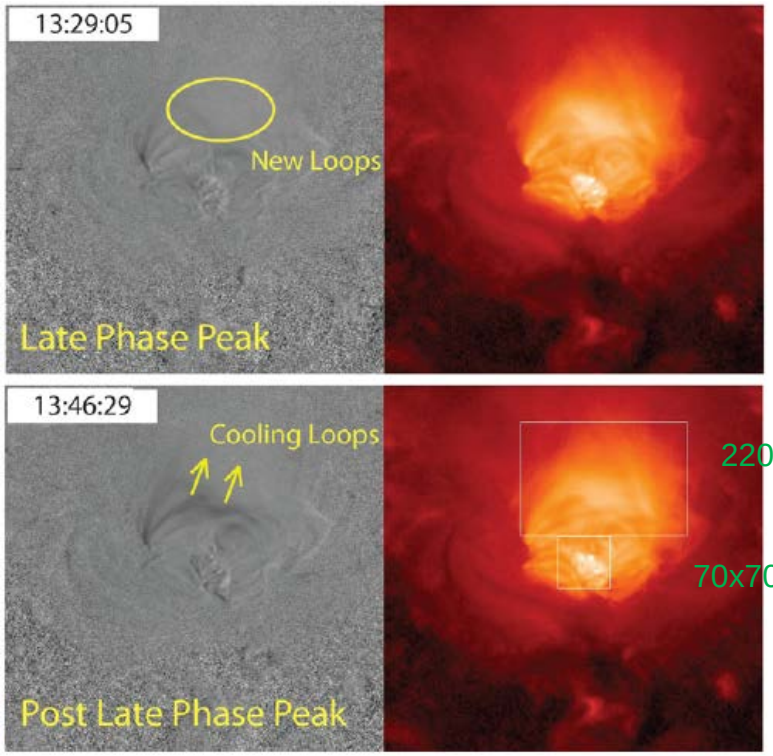


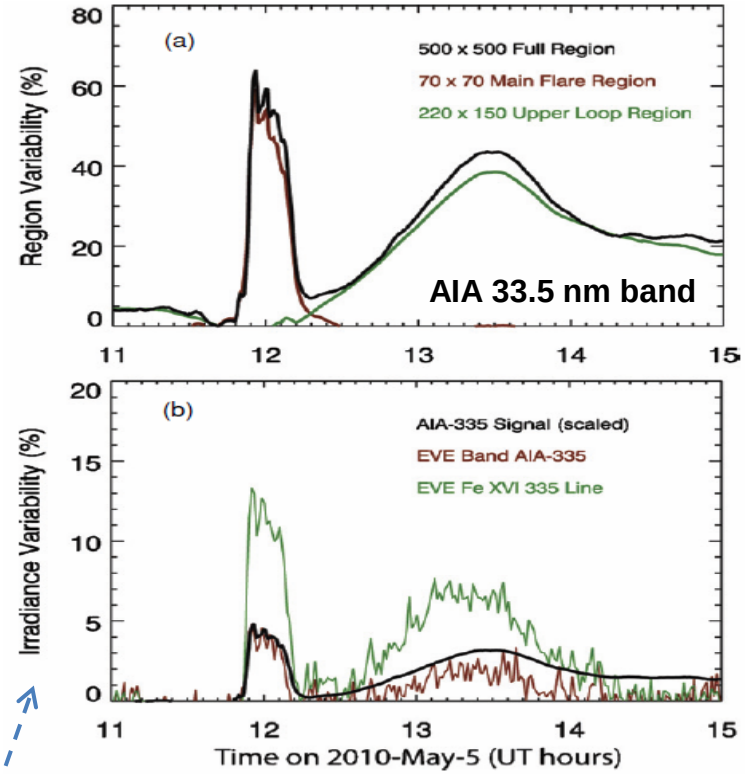


Time evolution of AIA Fe XVI 33.5 image for AR 11069 during C8.8 flare on 2010 May 5.
Left panel: difference images
Right panel: intensity images with logarithm color scale

**Variability= (Signal-Pre Flare level)/Pre Flare level**

Top panel: variability of AIA 33.5 nm band (full image, 500x500 pixels) in black, main flare region (70x70 pixels) in red and upper loop region (220x150 pixels) in green. Bottom panel: irradiance variability for EVE Fe XVI 33.5 nm line (green), EVE spectra convolved to AIA-335 (red) and AIA-335 (scaled signal, black).

*Woods et al., 2011, ApJ, 739*

# EVE and AIA video (5.05.2010 11÷15 UT)

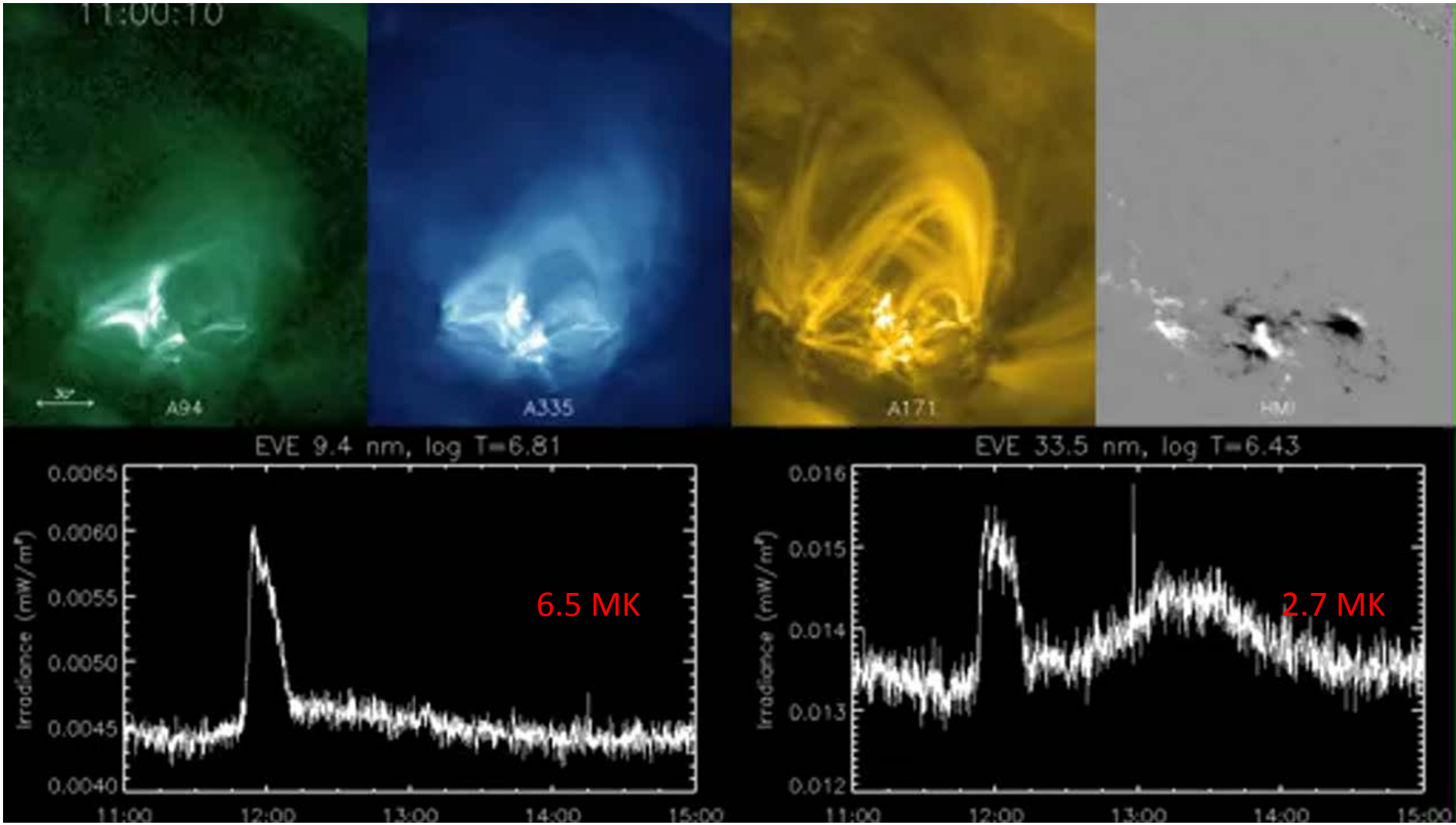

# Late phase flares

| Flare class | *GOES* | Analysed | Late phase |
|---|---|---|---|
| C1-C9 | 474 | 169 | 16 |
| M1-M9 | 46 | 21 | 9 |
| X1-X10 | 2 | 1 | 0 |
| Total | 522 | **191** | 25 |

Authors propose that the EUV late phase peak may have a similar physical origin as the main peak, but that the location and rate of reconnection are very different.

This later reconnection involves magnetic fields that arch high over the AR in the pre-eruption state, in contrast to the low-lying core fields that are involved in the main phase reconnection.

About half of the late phase flares are from **Ar 11069** in 2010 May and **AR 11121** in 2010 November → magnetic field configuration of AR appears to be important for EUV late phase.

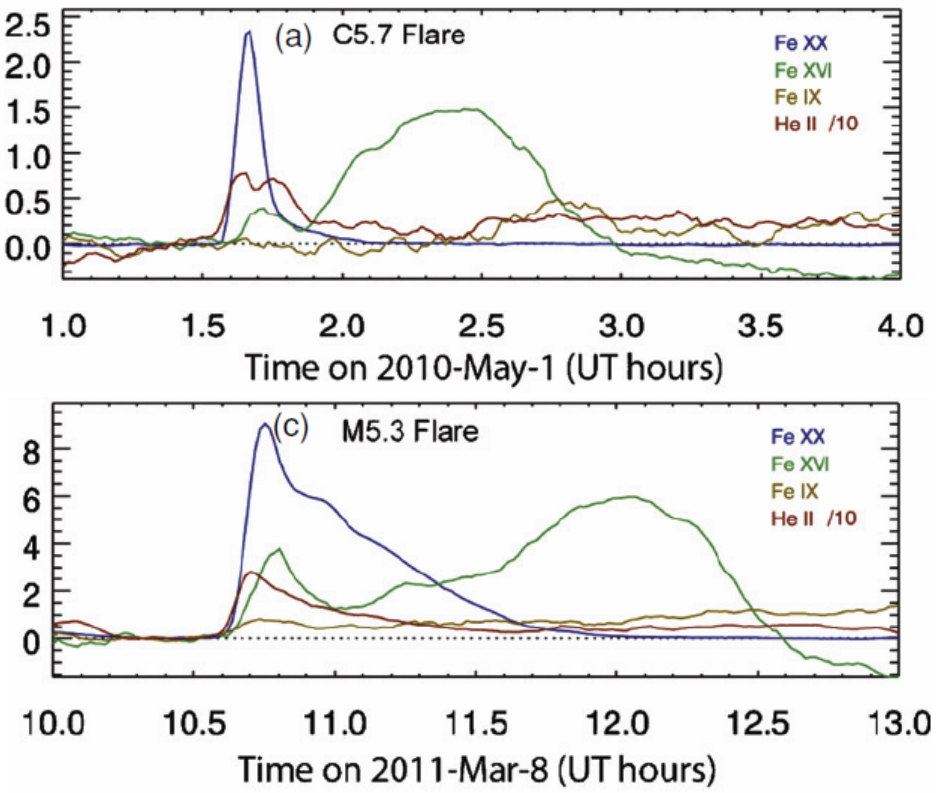


**Sometimes the EUV late phase emission is stronger than 1st peak emission.**

The second peak of Fe XVI emission occured between 41 and 204 minutes after the first peak, **an average delay of ~100 min.**
The ratio of second/ first peak: 0.2÷4.1, **average ratio ~0.8.**

*Woods et al., 2011, ApJ, 739*

# Comparison of AIA images and EVE lightcurves

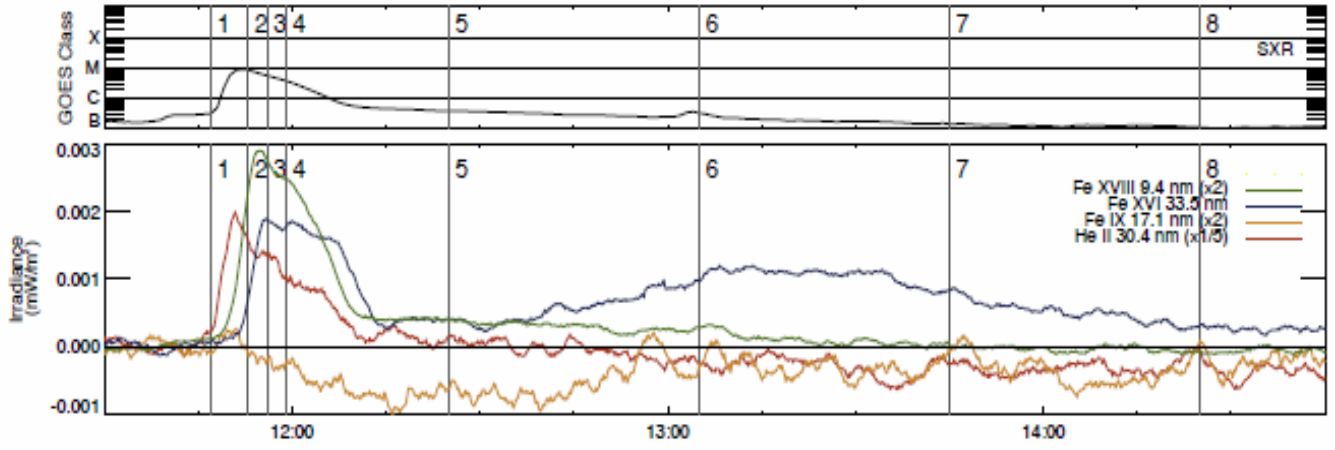


Fe XVIII , 9.4 nm
Fe XVI 33.5 nm, 3 MK
Fe IX 17.1 nm, 0.7 MK
He II 30.4 nm, ~0.08 MK (TR)

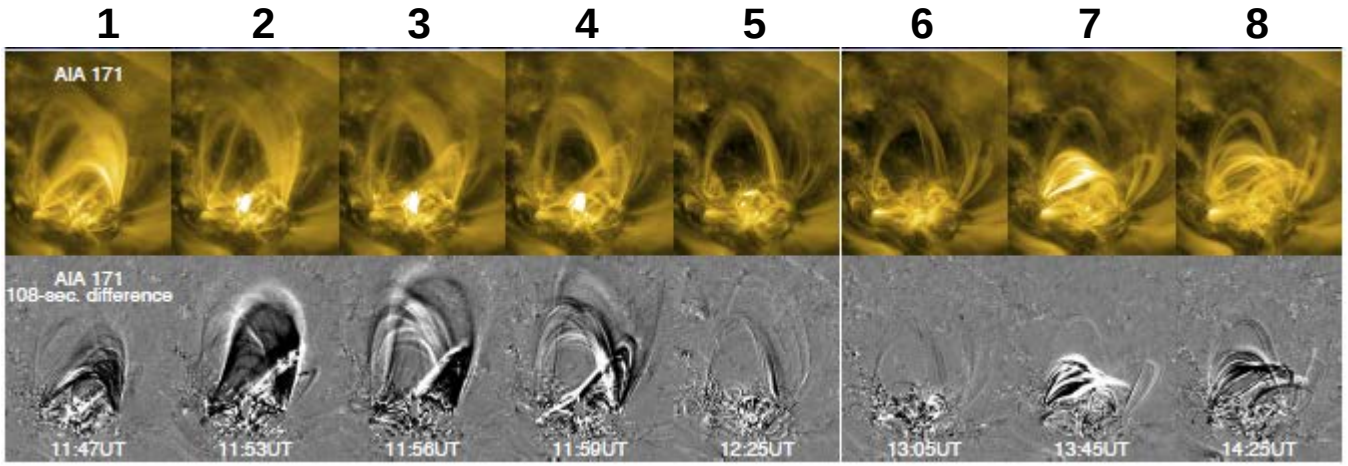


AIA 171 Å

difference images

AIA 171 Å→ morphology evolution of 5 May 2010 flare

*Hock, Woods, Klimchuk et al., 2012, ApJ*

# The origin of the EUV late phase

Comparison of AIA lightcurves constructing by summing the DN/s for every pixel in particular region (**entire AR**, **the core**, **overlying loops**) with EVE for dominant line in each AIA passband.

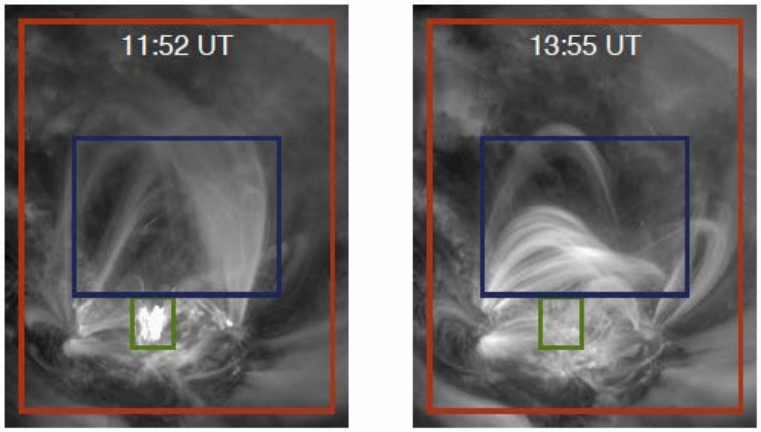


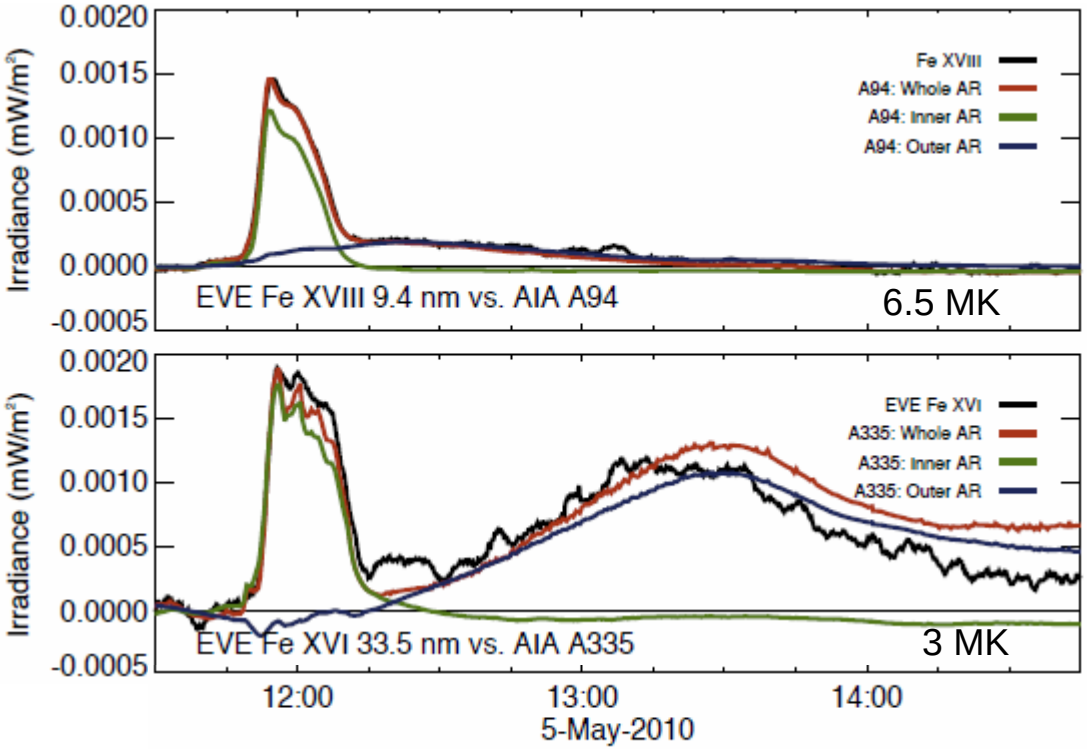


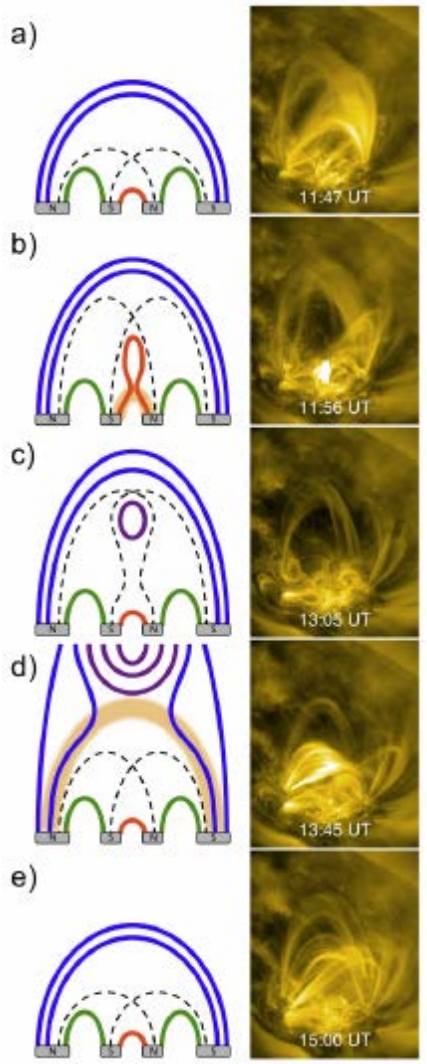


Pre-flare configuration

Main phase of the flare

Eruption and formation of CME

EUV late phase

Recovery to pre-flare configuration

Separatricis (boundary between **inner** and **outer** loops) denoted by dashed lines.

# Temperature (thermal) evolution plots

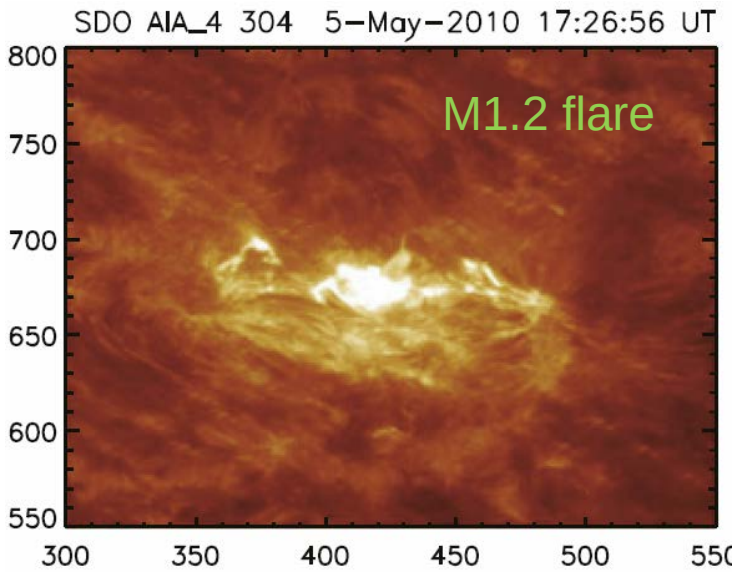


**Thermal (temperature) evolution plots:**

First to determine which emissions are isothermal and unblanded based on a characteristic formation temperature ($T_{max}$) of the associated contribution function G(T), from CHIANTI atomic database.

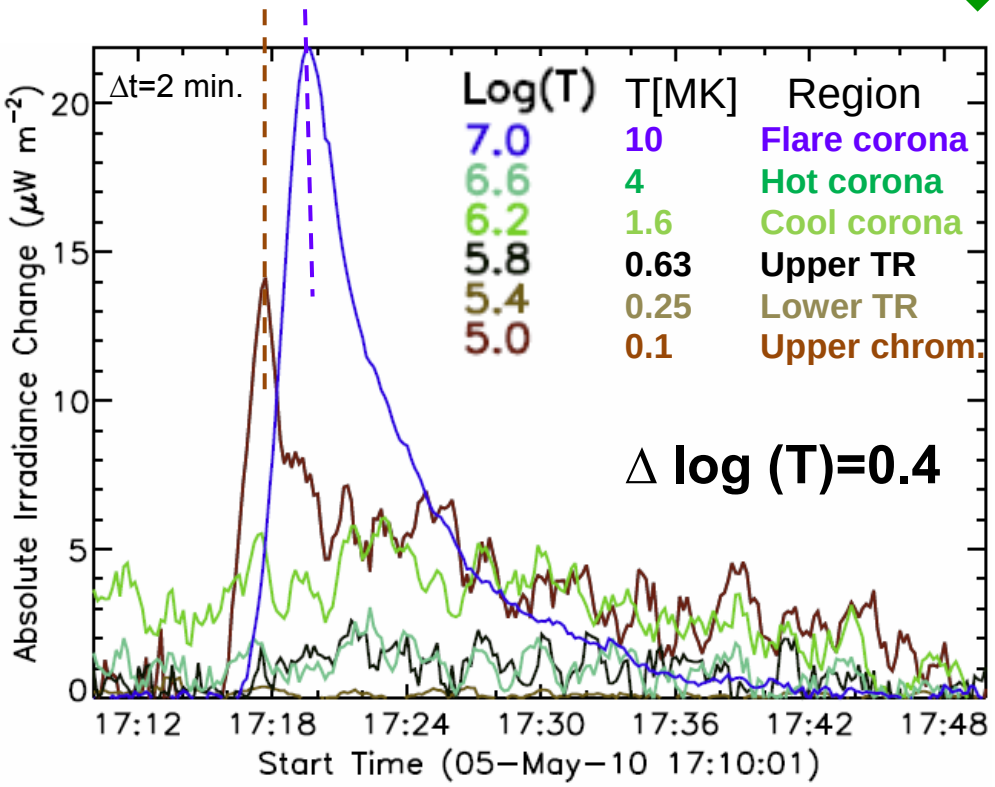


**Thermal evolution plot visualize the behaviour of plasma at different temperatures during flares**

An 8 min averaged pre-flare spectrum was subtracted.
A 30 s boxcar smoothing centered on each of 10 s EVE integrations was applied (noise reduced).
The flare-enhanced continua contributions were eliminated

*Chamberlin, Milligan and Woods, 2012, Solar Phys., 279*

# EVE: Fe XVIII and Fe XXII

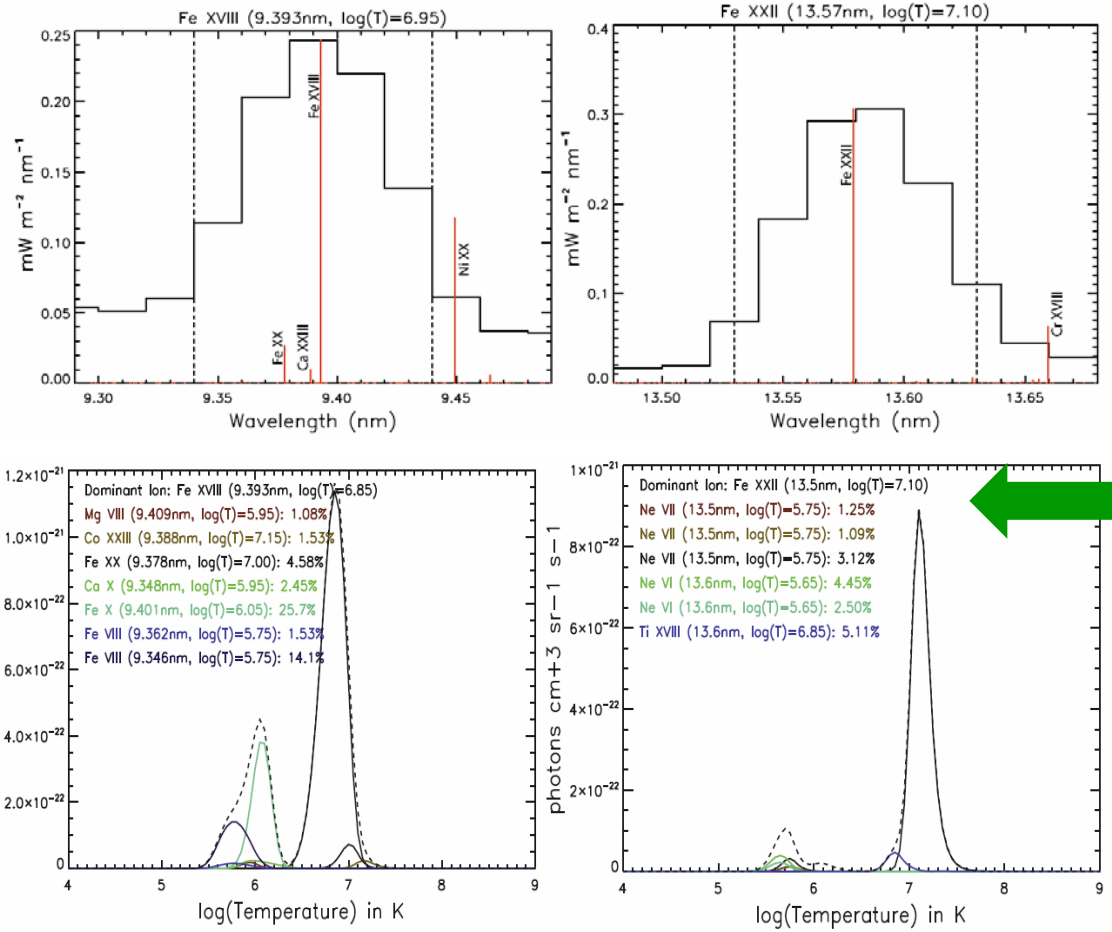


G(T) from CHIANTI centered on Fe XVIII and Fe XXII. Left 1 Å emission range is considered as **blended** (contribution of various species over a wide temp. range). Right: **unblended** (dominance of Fe XXII emission at T=1.26 MK)

**Measured EVE flare** spectrum (- the pre-flare spectrum), resolution (1Å) emission lines centered on Fe XVIII and Fe XXII.
**Red** contributions derived from CHIANTI assuming flare DEM and $N_e=10^{11}$ $cm^{-3}$.

Summed contribution functions for all emissions within 0.1 nm spectral ranhe →dashed black lines

Whether the line can be considered as isothermal (unblended) the **quality factor QF** is introduced:this is allowed percentage of total G(T) from all emission that lies outside $\log(T_{max}) \pm 0.15$

Here QF=0.3 meaning that up to 30% of the total G(T) for each 0.1 nm wide spectral line can come from outside the temperature range $\log(T_{max}) \pm 0.15$

*Chamberlin, Milligan and Woods, 2012, Solar Phys., 279*

# Absolute irradiance change: Δ log (T) = 0.1÷0.4

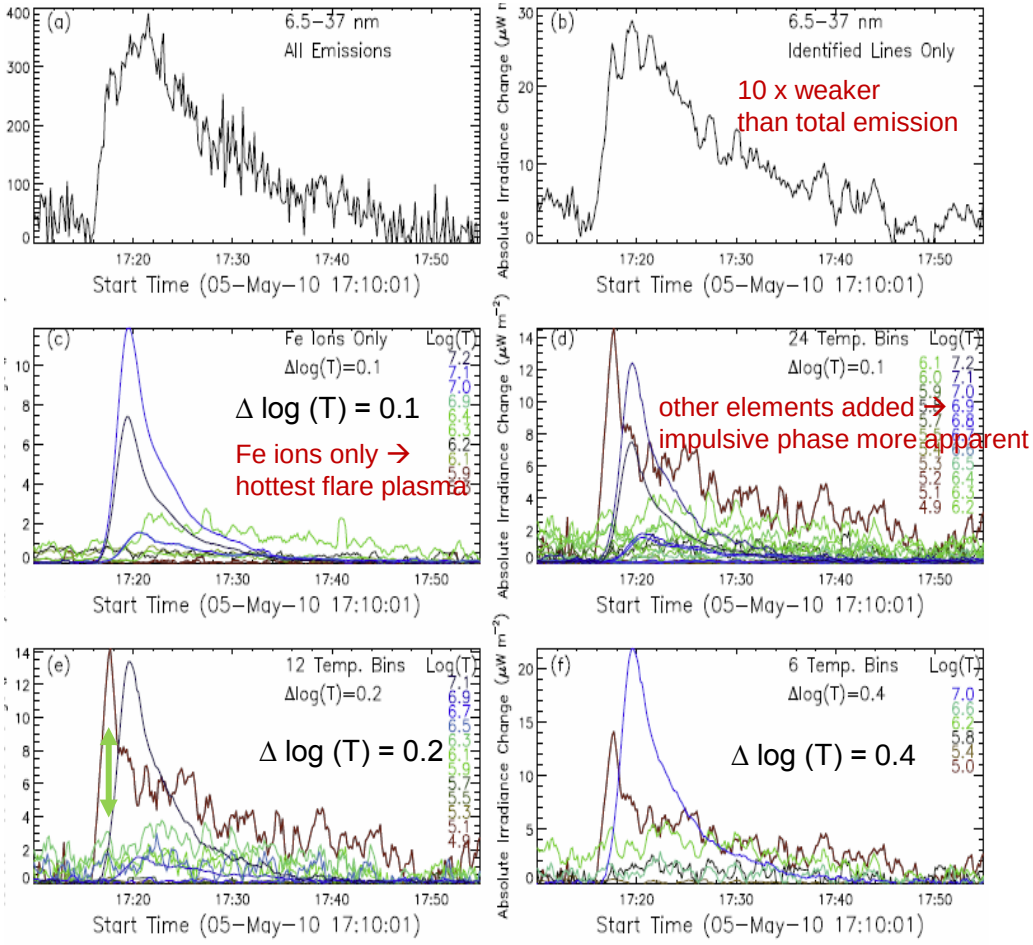


The code used to generate such plots (EVE_FLARE_TEMP_EVOL.PRO) is available through SolarSoft „EVE" branch – includes also subroutine (GET_EVE_DATA.PRO) for automatic download EVE data.

**b** → all unblended (isothermal) lines(QF=0.3)
**c** → dominated by hottest flare plasma, emission at lower temp. do not increase much above the pre-flare level until late in the flare, lack of Fe emission below 1 MK
**d** → Δ log (T) = 0.1; adding the emission from other elements makes the impulsive phase emission more apparent (He II 30.38 nm)
**e** → the same as **d** but Δ log (T) = 0.2, this reveals higher temp. synchronized with He II emission
**f** → hot emission dominates due to addition of high-temp. lines

5 flares analysed

*Chamberlin, Milligan and Woods, 2012, Solar Phys., 279*

# 2011 Feb. 24 M3.5 limb flare

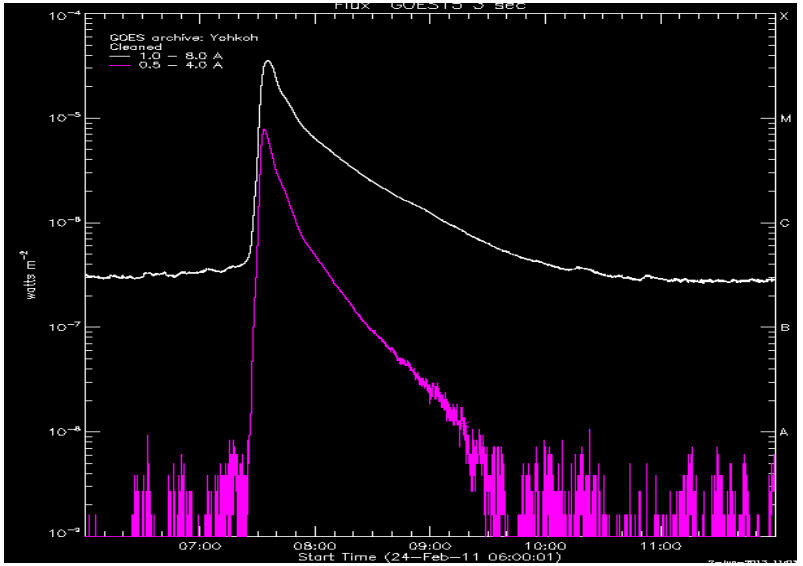


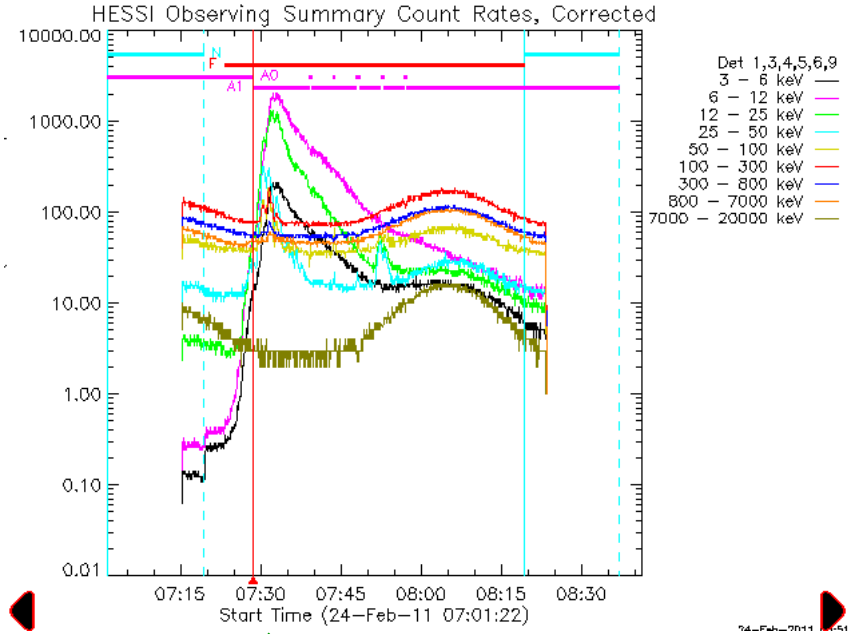


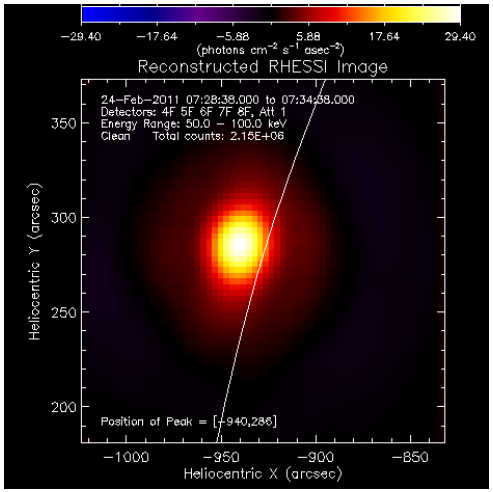

# *RHESSI* and *SDO*/AIA observations

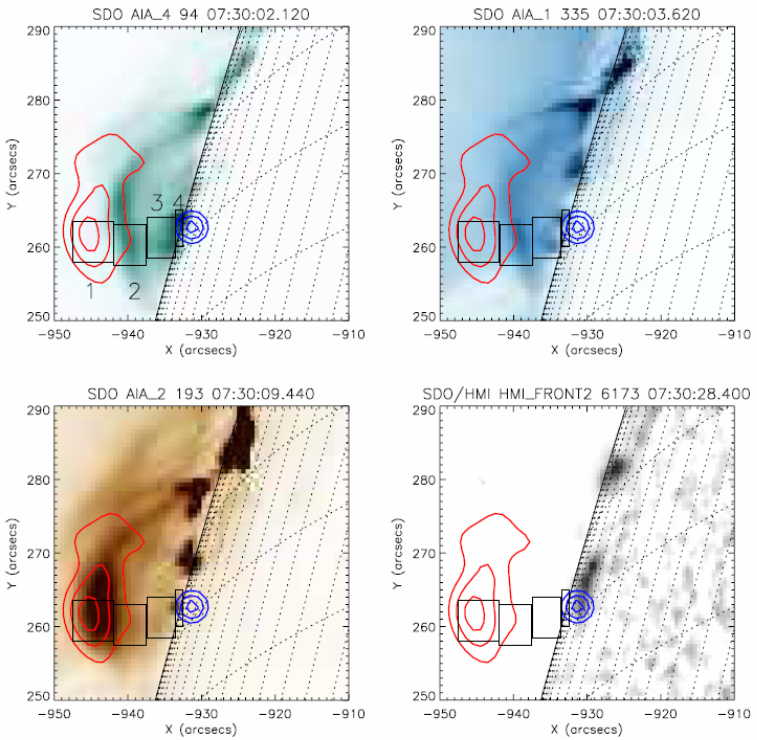


AIA images (94, 335, 193 Å and HMI difference white-light image) overlaid with *RHESSI* **thermal emission** (red contours in CLEAN image) and **non-thermal emission** (blue contours). The rectangles indicate the regions of interest on which the analysis is focused.
Loop-top 193 Å emission cospatial with *RHESSI* while other „hot" emission (94 Å channel) is NOT. Loops visible in 94 Å are ~5" lower than 193 Å structure.

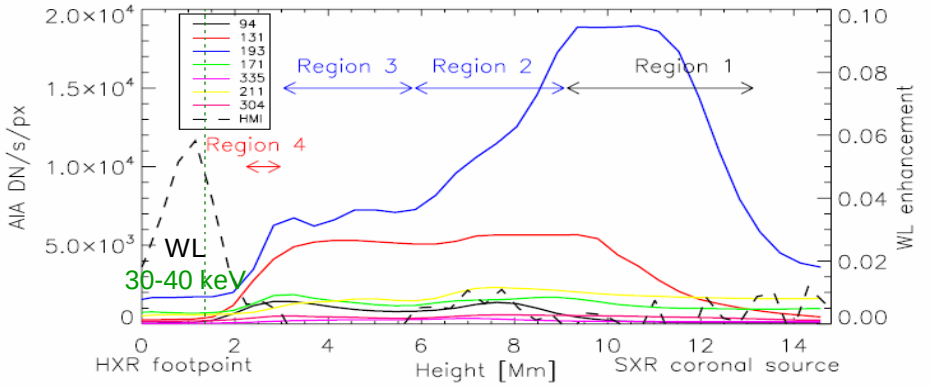


Profiles of AIA maps as a function of height above the photosphere: along the x direction averaged over 6" in y-direction

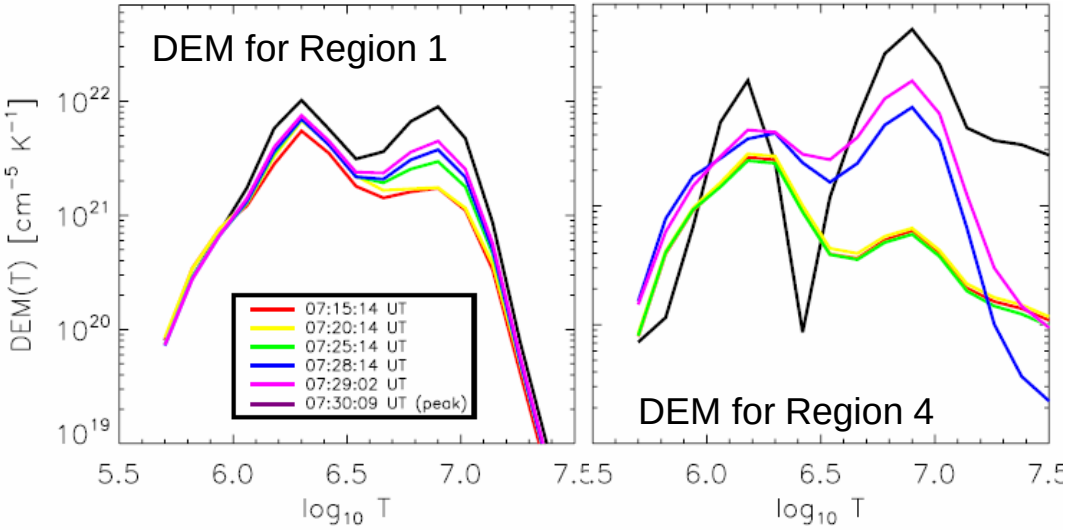


**2 MK** (low temp. component) attributed to line-of-sight effect -seen in all 4 regions and weakly changing with time
**8 MK** component dominates the flare emission → $N_e$=2.4 $10^{10}$ cm $^{-3}$

*Battaglia and Kontar, 2012, ApJ, 760*

# Cross-field temperature distributions

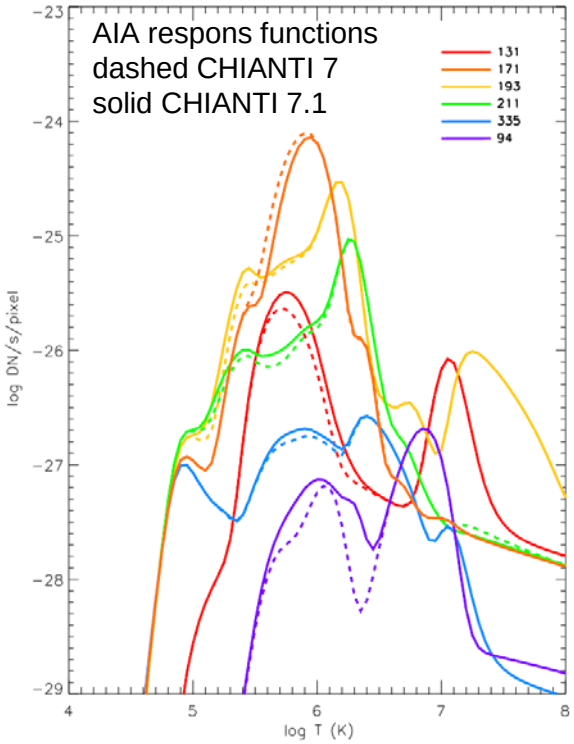


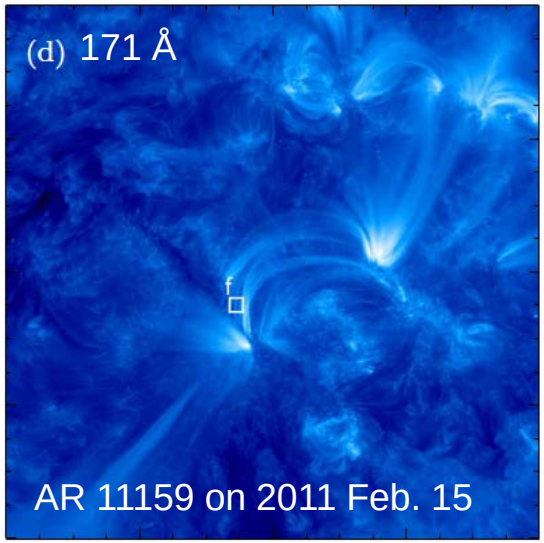


DEMs for loop segments + 100 Monte-Carlo realizations:

- used 6 AIA coronal filters (Fe VIII 131Å, Fe IX 171Å, Fe XII 193Å, Fe XIV 211Å, Fe XVI 335Å, Fe XVIII 94Å)
- new atomic data (solid lines - CHIANTI 7.1)
- *XRT_dem_iterative2 routine* (allows Monte-Carlo iterations: observed intensity in each filter is varied randomly using a gaussian distribution- observed intensity is the centroid and the uncertainty is the width)
- **12 beckground subtracted loop segments** from **6 active regions**.

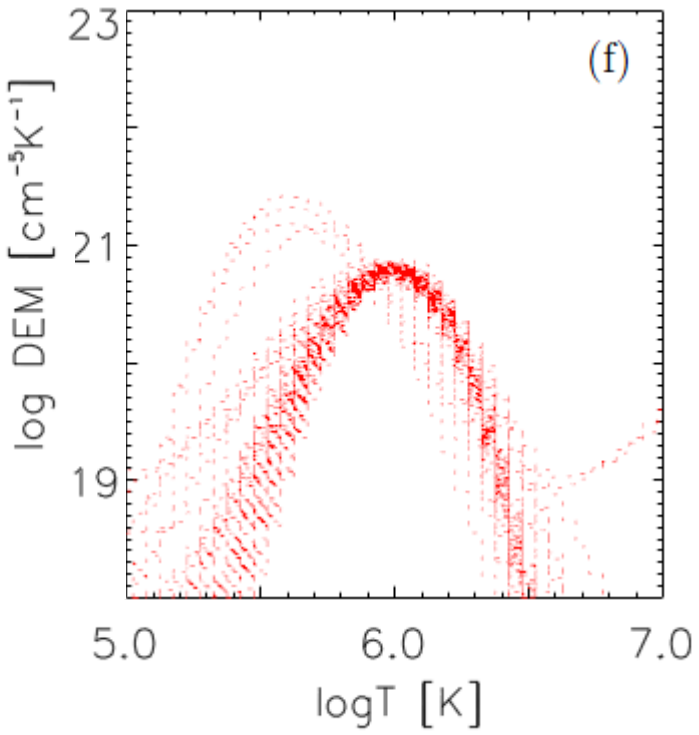


The resulting temperature distributions are **NOT** consistent with isothermal plasma.
The observed loops can not be modelled as single flux tubes and must be composed of a collection of magnetic strands. ← supported by Cirtain, Golub, Winebarger, et al., Energy release in the solar corona from spatially resolved magnetic braids, Nature, 493, 501, 2013

*Schmelz, Jenkins, and Pathak, 2013, ApJ, 770*

# High-resolution Coronal Imager (Hi-C)

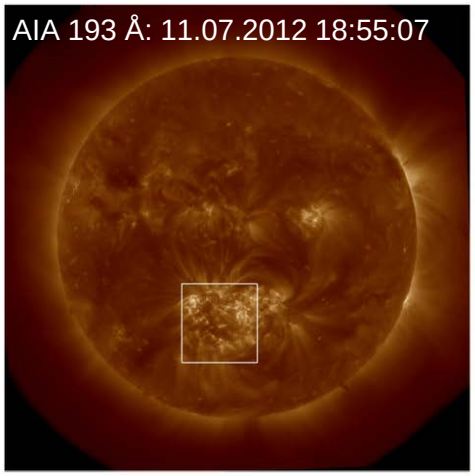


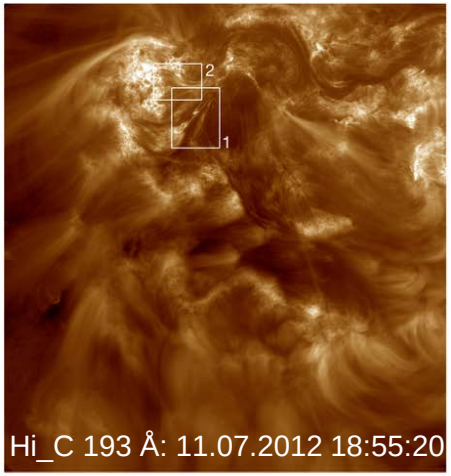


**Hi-C** was launched on a sounding rocket on 11 July 2012 and took images of the 1.5 MK coronal plasma with a resolution of 0.2 ” (~ 150 km) for 5 minutes. The Hi-C passband isolates a very narrow window in the EUV, centered at 193 Å (Fe XII lines). AIA has an identical channel that images the full solar disk.

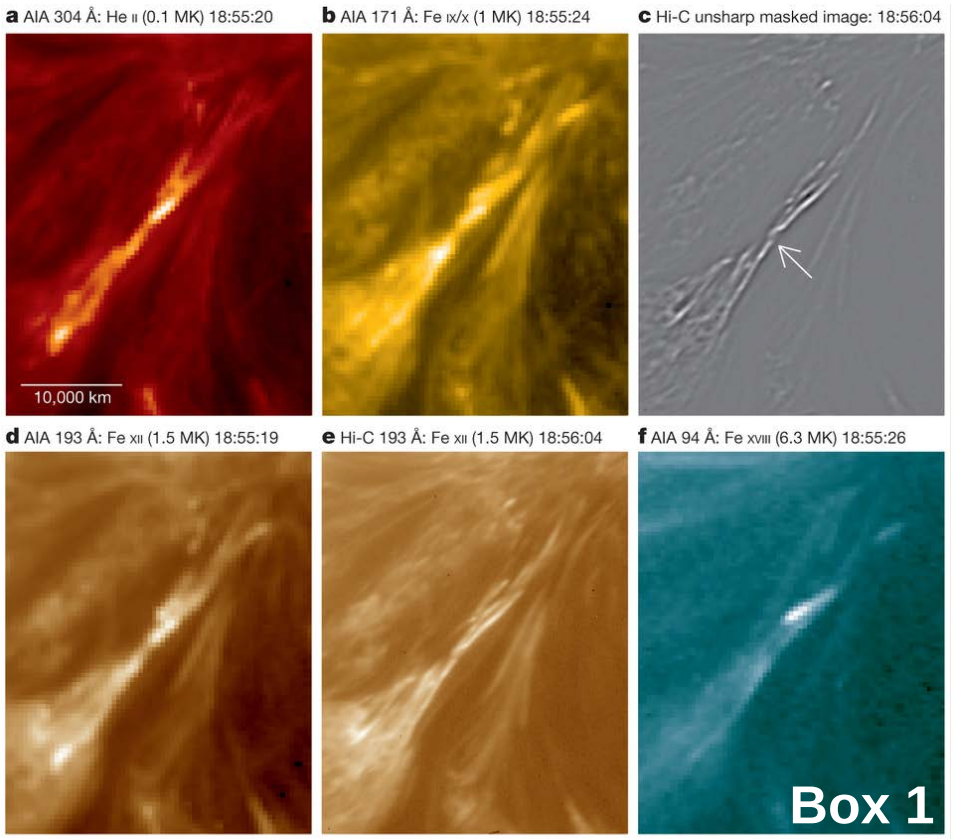


**A coronal loop seen at several different coronal temperatures by AIA and Hi-C**: Labels indicate the passbands, the dominant emitting ion and the peak formation temp. of the ion. The image in **c** was constructed by smoothing the original image (**e**) and subtracting the processed image from the original →enhancement of the shapes of fine-scale structures in the image. All panels show a narrow magnetic arch that Hi-C resolves to be twisted along its length. The twisted loops converge and appear to intersect (**arrow in c**).

**A C1.7 flare centered on this intersection is seen in the AIA images about 3 min after the Hi-C flight.**

*Cirtain, Golub, Winebarger et al., 2013, Nature, 493*

# Time series from Hi-C (**Box 2**)

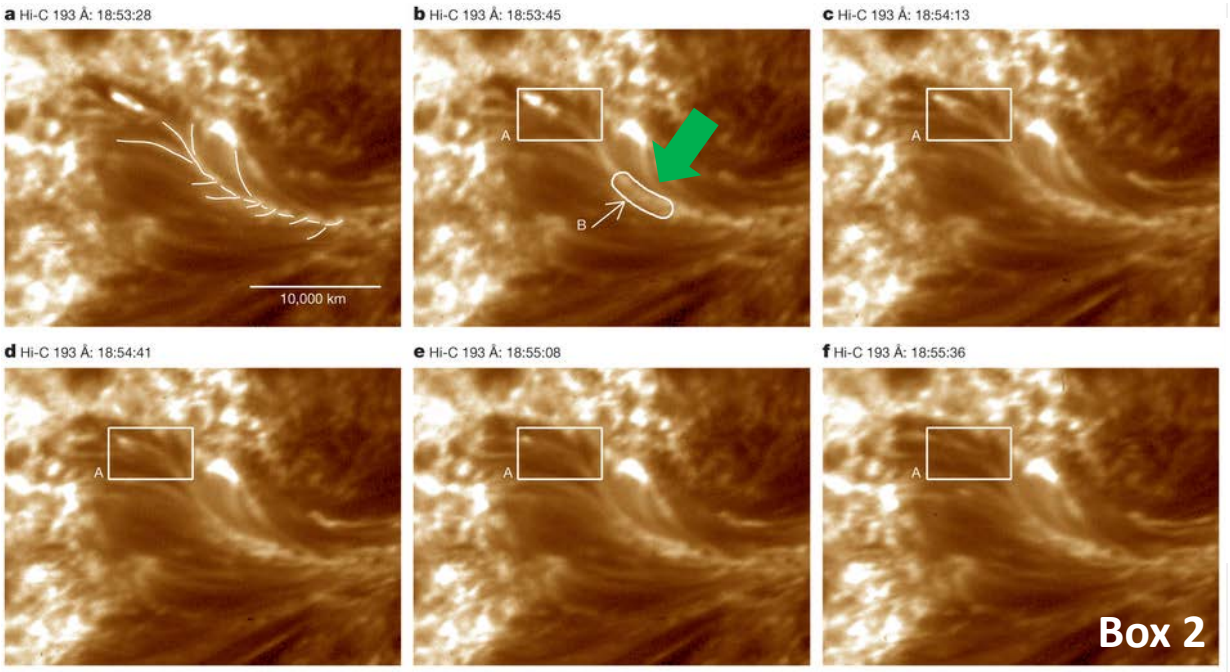


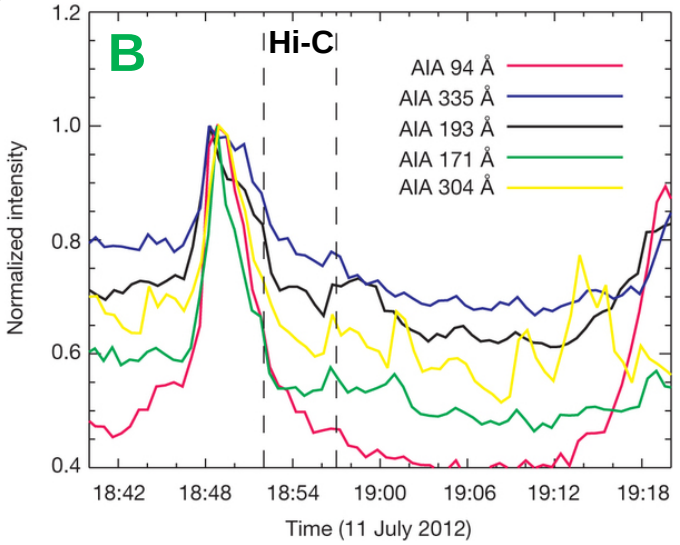


This braided (not simply twisted) bundle of loops (magnetic fields), *seen in the AIA data as a single loop*, is observed for over 12 h and brightens repeatedly over the AIA observation period.
By reconnecting, presumably at current sheets between entwined flux strands, the brided loops release energy into the corona.
The braiding is driven by the ubiquitous small-scale, convection-driven motion of the photospheric feet of the magnetic field.

The light curves from multiple AIA channels for **area B** show the increase in intensity for the braided ensemble of loops just before the Hi-C flight. **The heating process shown here repeats several times per hour over the 12 or more hours the structure is present in the AIA data.**

Total free energy estimated based on magnetic field ~$10^{29}$ erg
The radiated energy from the AIA lightcurves is ~$10^{26}$ erg

*Cirtain, Golub, Winebarger et al., 2013, Nature, 493*

# Video: Nature